Available online at www.sciencedirect.com
ScienceDirect
Sensors and Actuators A 138 (2007) 384–393
SENSORS AND ACTUATORS A PHYSICAL
www.elsevier.com/locate/sna

Electromechanical coupling in dielectric elastomer actuators

Michael Wissler [a,b,*], Edoardo Mazza [b,c]

[a] *Empa, Swiss Federal Laboratories for Materials Testing and Research, Laboratory for Materials and Engineering, Überlandstrasse 129, CH-8600 Dübendorf, Switzerland*
[b] *ETH, Swiss Federal Institute of Technology, Department of Mechanical Engineering, CH-8092 Zürich, Switzerland*
[c] *Empa, Swiss Federal Laboratories for Materials Testing and Research, Laboratory of Mechanics for Modelling and Simulation, Überlandstrasse 129, CH-8600 Dübendorf, Switzerland*

Received 18 August 2006; received in revised form 8 March 2007; accepted 25 May 2007
Available online 2 June 2007

Abstract

In this paper the electromechanical coupling in dielectric elastomer actuators is investigated. An equation proposed by Pelrine et al. [R.E. Pelrine, R.D. Kornbluh, J.P. Joseph, Electrostriction of polymer dielectrics with compliant electrodes as a means of actuation, Sens. Actuators A 64 (1998) 77–85] is commonly used for the calculation of the electrostatic forces in dielectric elastomer systems. This equation is analyzed here with (i) energy consideration and (ii) numerical calculations of charge and force distribution. A new physical interpretation of the electrostatic forces acting on the dielectric elastomer film is proposed, with contributions from in-plane and out-of-plane stresses. Representation of this force distribution using Pelrine's equation is valid for an incompressible material, such as the acrylic elastomer VHB 4910.

Experiments are performed for the measurement of the dielectric constant ε_r of the acrylic elastomer VHB 4910 for different film deformations. The values of ε_r are shown to decrease with increasing pre-stretch ratio λ_p, from 4.7 for the un-stretched film, down to 2.6 for equi-biaxial deformation with $\lambda_p = 5$. This result is important in that it corrects the constant value of 4.7 largely applied in literature for pre-stretched dielectric elastomer actuator modeling. With the results of this work the predictive capabilities of a model describing the three-dimensional passive and active actuator behavior are remarkably improved.

Keywords: Electromechanical coupling; Dielectric elastomer; Dielectric constant; Actuator; Modeling

1. Introduction

Actuators made of dielectric elastomers (DE) consist of a compliant capacitor, with a thin soft elastomer film sandwiched between two compliant electrodes [1,2]. Application of a voltage leads to electrostatic forces that deform the elastomer membrane, which contracts in the thickness direction and expands in the film plane. This in-plane expansion is exploited to generate motion or forces. Dielectric elastomers actuators transform electrical energy directly into mechanical work and are able to generate in-plane deformations of up to 30% with respect to the un-activated configuration. They belong to the group of so called electroactive polymers (EAP).

Modeling and simulation of DE systems are key steps in the design and optimization of DE actuators. Challenges thereby are represented by the description of (i) the passive mechanical behavior of the elastomers (with large strains, time and history dependence of the mechanical response) and (ii) the mechanical forces generated by the electric field, i.e. what is often referred to as "electromechanical coupling". Significant work has been performed for the mechanical characterization of the elastomers [3–8], whereas only few papers exist on electromechanical coupling.

Electromechanical coupling is commonly described using a model proposed by Pelrine et al. [1]. In this model electrostatic forces are assumed to act in the direction perpendicular to the insulating elastomer film, and their magnitude is characterized

* Corresponding author at: Empa, Swiss Federal Laboratories for Materials Testing and Research, Laboratory for Materials and Engineering, Überlandstrasse 129, CH-8600 Dübendorf, Switzerland. Tel.: +41 44 823 4787; fax: +41 44 823 4011.
E-mail addresses: michael.wissler@empa.ch, mtwissler@hotmail.com (M. Wissler).

0924-4247/$ – see front matter © 2007 Elsevier B.V. All rights reserved.
doi:10.1016/j.sna.2007.05.029

by p_{el}, the so called "electrostatic pressure". p_{el} is calculated for a given applied voltage U and film thickness z as

$$p_{el} = \varepsilon_0 \varepsilon_r \frac{U^2}{z^2} = \varepsilon_0 \varepsilon_r E^2 \quad (1)$$

Thereby, ε_0 is the free-space permittivity (8.854×10^{-12} A s/V m), ε_r the elastomer dielectric constant and E is the electric field.

Eq. (1), which will be referred to as "Pelrine's equation" in this paper, has been derived for free boundary conditions and is generally accepted as representing the electromechanical coupling in dielectric elastomer systems. Kofod and Sommer-Larsen [4] validated the equation for silicone experimentally. To our knowledge, no comprehensive analysis of this expression has been presented so far.

The present investigations on electromechanical coupling are mainly motivated by inconsistent results obtained from uniaxial mechanical tests and DE actuator experiments recently presented in [8]. We reported there on an extensive experimental characterization of so called "circular actuators" made of VHB 4910 (an acrylic elastomer produced by 3 M) with tests over a wide pre-strain and voltage range. Visco-hyperelastic constitutive equations were used to describe the response of the elastomer. The parameters of the mechanical model were determined from the results of circular actuators experiments with radial pre-stretch ratios $\lambda_p = 3$, 4 and 5 (the pre-stretch ratio λ_p is defined as the ratio between radius of the circular actuator after and before stretching) at a constant voltage of 2 kV. Fig. 1a shows the comparison between simulation and experimental results for the model using the Arruda–Boyce strain energy formulation [9]. Electromechanical coupling was thereby described by Eq. (1) and a value of 4.7 was used for the dielectric constant of VHB 4910, according to [10,11]. Despite the good predictive capabilities of the model for the circular actuator test, the constitutive equations failed to describe the passive uniaxial response, with significant discrepancy between data points from tensile and relaxation experiments and the corresponding simulations, Fig. 1b.

Describing the mechanical behavior over a wide range of stress and deformation states represents a common challenge for three-dimensional constitutive equations. We therefore concentrated first on the mechanical model formulation when searching for the causes of this inconsistency. The corresponding exercises using different strain energy formulations (with the strain energy functions of Yeoh [12] and Odgen [13] in addition to that of Arruda–Boyce) failed to overcome the inconsistency. We then focused our attention on the electromechanical coupling model, thereby questioning (i) the general validity of Eq. (1), and more specifically (ii) the adopted value of 4.7 for the dielectric constant ε_r. The results of these investigations are reported in this paper.

In Section 2 we analyze Pelrine's equation for the case of a circular actuator. In a first step an energy balance is formulated which includes the energy from the power source, the energy of the electrical field and the mechanical energy. In a second step, the charge and the forces distributions on a circular actuator are calculated numerically. In Section 3 the dielectric constant is determined for VHB 4910 with two different approaches: (i) the dielectric constant is measured using a capacitor set-up, at different pre-strain levels ($\lambda_p = 1$, 3, 4 and 5) and frequencies (100 Hz and 10 kHz); (ii) the electromechanical forces and thus the corresponding dielectric constant are measured in experiments with a spring roll actuator. This test is similar to an experiment ('blocking force experiment') proposed by Kofod et al. [4,11] for measuring the dielectric constant. The results of these investigation and their implications for DE actuator models (in particular concerning the inconsistency illustrated in Fig. 1) are discussed in Section 4.

2. Electromechanical coupling

A circular actuator consisting of a dielectrica (elastomer) and two electrodes (Fig. 2) is selected as electromechanical system. The following assumptions hold for this analysis: (i) electrostrictive effects are negligible [11], (ii) the electrodes are assumed to be ideally compliant (they do not constrain the elastomer mechanically) and (iii) the elastomer is incompressible.

2.1. Energy considerations

A closed system including the circular actuator is considered (Fig. 2). Application of a voltage U leads to a charge Q on

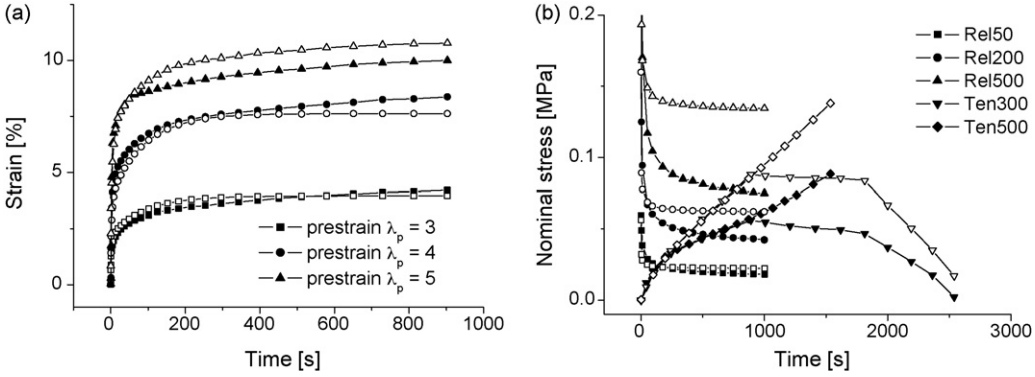

Fig. 1. Experiment vs. simulation for (a) circular actuator tests at $\lambda_p = 3$, 4 and 5, and (b) uniaxial experiments with three relaxation tests (Rel50, Rel200 and Rel500) and two tensile tests (Ten300 and Ten500) [8]. The filled symbols represent the experimental data and the open symbols the corresponding simulations.

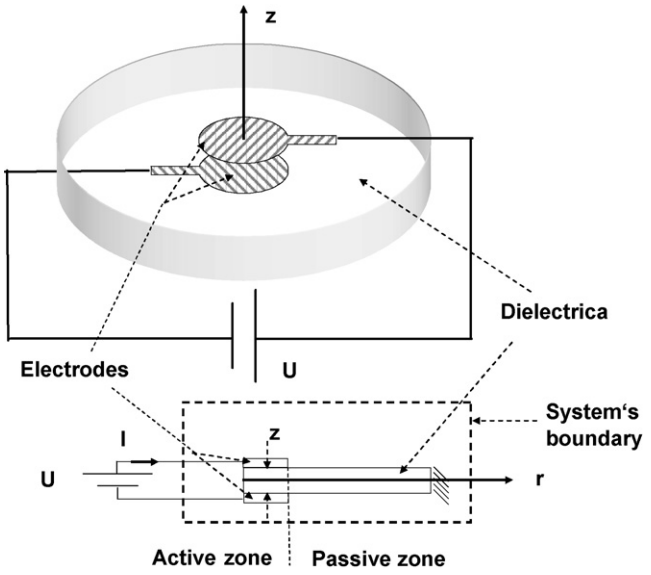

Fig. 2. Sketch of the considered electromechanical system. The film thickness z is indicated.

the electrodes. The time rate of change of Q correspond to the current I. Charge Q on the electrodes and voltage U are linked. Most energy considerations in literature are formulated by either a constant voltage or a constant charge [1]. This corresponds to a usual approach to calculate forces of plate capacitors. In the present analysis charge and voltage are described as variables dependent on the deformation of the elastomer film. For the present configuration the deformation consists in equi-biaxial in-plane extension and the corresponding out-of-plane contraction. For an incompressible material (volume is constant) this deformation can be described by the film thickness z. U and Q are therefore handled as functions of z.

Three energy forms are considered for the energy balance: the energy from the electrical power source W_{ext}, the energy of the electric field W_{el} and the mechanical energy W_{m}. All three energies are dependent on the thickness z. The energy balance for the closed electromechanical system for an incremental deformation $\mathrm{d}z$ is given by the following equation:

$$\frac{\mathrm{d}W_{\text{ext}}(z)}{\mathrm{d}z} = \frac{\mathrm{d}W_{\text{el}}(z)}{\mathrm{d}z} + \frac{\mathrm{d}W_{\text{m}}(z)}{\mathrm{d}z} \tag{2}$$

In the following W_{ext}, W_{el} and W_{m} are determined. The time derivative of the energy from the power source is related to current I and voltage U, as

$$\frac{\mathrm{d}W_{\text{ext}}}{\mathrm{d}t} = UI = U\frac{\mathrm{d}Q}{\mathrm{d}t} \tag{3}$$

where t is the time. Considering $z(t)$ and applying the chain rule leads to

$$\frac{\mathrm{d}W_{\text{ext}}}{\mathrm{d}z} = U(z)\frac{\mathrm{d}Q(z)}{\mathrm{d}z} \tag{4}$$

Q and U are linked as $Q(z) = C(z)U(z)$ with the capacitance C defined here as

$$C = \frac{\varepsilon_0\varepsilon_{\text{r}}A}{z} = \frac{\varepsilon_0\varepsilon_{\text{r}}V_0}{z^2} \tag{5}$$

where A is the area coated by the electrodes and V_0 is the elastomer volume (Az) of the active zone, which remains constant during deformation. $\mathrm{d}Q/\mathrm{d}z$ can thus be expressed as:

$$\frac{\mathrm{d}Q(z)}{\mathrm{d}z} = \varepsilon_0\varepsilon_{\text{r}}V_0\frac{\mathrm{d}}{\mathrm{d}z}\left(\frac{U(z)}{z^2}\right) = \frac{\varepsilon_0\varepsilon_{\text{r}}V_0}{z^2}\left(\frac{\mathrm{d}U}{\mathrm{d}z} - 2\frac{U}{z}\right) \tag{6}$$

$\mathrm{d}W_{\text{ext}}/\mathrm{d}z$ is given by the combination of Eqs. (4) and (6):

$$\frac{\mathrm{d}W_{\text{ext}}}{\mathrm{d}z} = \frac{\varepsilon_0\varepsilon_{\text{r}}V_0U}{z^2}\left(\frac{\mathrm{d}U}{\mathrm{d}z} - 2\frac{U}{z}\right) \tag{7}$$

The rate of change of the energy of the power source depends on the rate of change of the voltage. The energy W_{el} stored by the electric field in a capacitor is

$$W_{\text{el}} = \tfrac{1}{2}CU^2 \tag{8}$$

by inserting C from Eq. (5) the derivative $\mathrm{d}W_{\text{el}}/\mathrm{d}z$ results:

$$\frac{\mathrm{d}W_{\text{el}}}{\mathrm{d}z} = \frac{1}{2}\varepsilon_0\varepsilon_{\text{r}}V_0\frac{\mathrm{d}}{\mathrm{d}z}\left(\frac{U(z)^2}{z^2}\right) = \frac{\varepsilon_0\varepsilon_{\text{r}}V_0U}{z^2}\left(\frac{\mathrm{d}U}{\mathrm{d}z} - \frac{U}{z}\right) \tag{9}$$

Note that also $\mathrm{d}W_{\text{el}}/\mathrm{d}z$ depends on $\mathrm{d}U/\mathrm{d}z$. Eqs. (9), (7) and (2) lead to the following result for the derivative of the mechanical energy $\mathrm{d}W_{\text{m}}/\mathrm{d}z$:

$$\frac{\mathrm{d}W_{\text{m}}}{\mathrm{d}z} = -\frac{\varepsilon_0\varepsilon_{\text{r}}V_0U^2}{z^3} \tag{10}$$

The basic assumption of Pelrine's model is that electrostatic forces are homogeneously distributed over the coated area $A = V_0/z$ and act in z direction. The mechanical energy represents the work of the external (electrostatic) forces on the film. With the assumption that $\mathrm{d}W_{\text{m}}/\mathrm{d}z$ is the total external force, the corresponding pressure p_z is obtained as:

$$p_z = -\frac{\mathrm{d}W_{\text{m}}}{\mathrm{d}z}\frac{1}{A} = \varepsilon_0\varepsilon_{\text{r}}\left(\frac{U}{z}\right)^2 \tag{11}$$

This result confirms Pelrine's equation, when comparing p_z with p_{el} from Eq. (1). Pelrine et al. refer to the contribution of lateral and out-of-plane effects, included in Eq. (3) in [1]. By the definition of the pressure p_z (Eq. (5) in [1] and Eq. (11) in this work) the presence of forces acting only in z-direction is assumed. The influence of radial ("lateral") electrostatic forces [1,14] can be determined with a direct calculation of charge and electrostatic force distributions. To this end, for the configuration shown in Fig. 2, a corresponding numerical calculation has been carried out and is described in the next section.

2.2. Charge and force distributions

The simulation program COMSOL Multiphysics [15] has been used for the present calculations. An axisymmetric model of a circular actuator (element type: 'Lagrange-quadratic') including a dielectrica and two electrodes has been created, Figs. 3 and 4. The electrodes are assumed to have straight edges. The following geometrical parameters are used, Fig. 3: the thickness of the dielectrica is $z_{\text{d}} = 60\,\mu\text{m}$, this corresponds to a VHB 4910 actuator pre-stretched by a factor of approximately $\lambda_{\text{p}} = 4$.

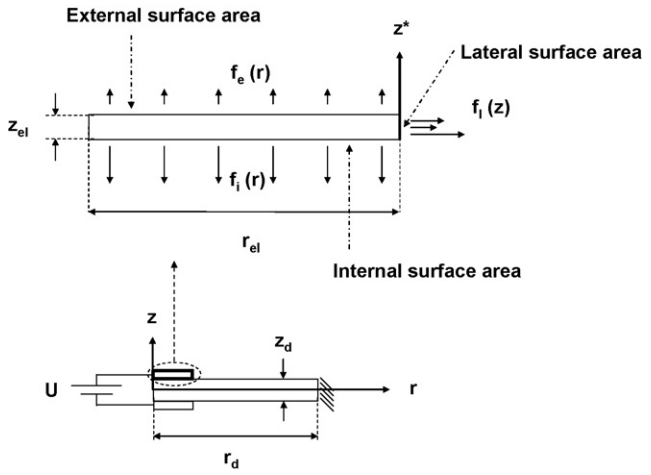

Fig. 3. Sketch of the COMSOL Mulitphysics model. For the electrode, the coordinates r, z and z^* are introduced for later reference.

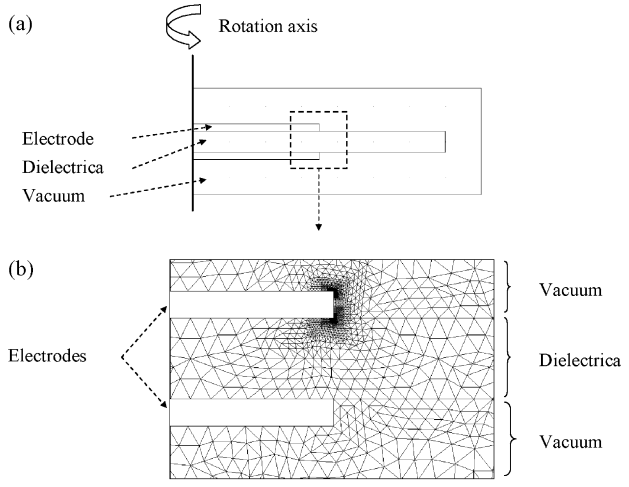

Fig. 4. (a) Sketch of the COMSOL Multiphysics model and (b) meshing of the part indicated in (a).

The radius of the dielectrica is $r_d = 14$ mm. The radius of the electrode is $r_{el} = 7$ mm and the thickness of the electrode is $z_{el} = 20$ μm. Microscopic investigations showed that $z_{el} = 20$ μm is a reasonable value for a hand-applied graphite powder/silicone oil electrode.

The dielectric constant of the dielectrica was chosen as $\varepsilon_r = 4.7$. For the bordering empty space the dielectric constant of vacuum $\varepsilon_r = 1$ was used. As boundary condition a potential difference of $U = 3$ kV has been applied between the electrodes. Since the electrodes are conductive, all the charges are on the surface area of the electrodes: the so called internal surface area, lateral surface area and external surface area, indicated in Fig. 3. The mesh is shown in Fig. 4. Singularities at corners have been closely investigated at the upper electrode with a strong mesh refinement at the corresponding locations.

All electric field variables (electric potential, electric field, surface charge density ρ_s) are calculated by solving Poisson's equation numerically. On the rotational axis a suitable symmetry boundary condition is applied. Further information on the numerical calculation can be found in [15].

The surface charge density of the internal surface area $\rho_i(r)$ and the surface charge density of the lateral surface area $\rho_l(z^*)$ are shown in Fig. 5. The surface charge density of the external surface area is neglected because there is no charge on this surface except at the right corner, with a singularity which does not influence the electromechanical behavior.

The charges on the electrodes cause electrostatic forces. These forces are parallel to the electric field. Both forces and electric field vectors are perpendicular to the electrode's surface area. The calculated electric field distribution is qualitatively represented in Fig. 6.

The electrostatic forces are described by Maxwell's stress tensor t_{ij}^{M} [16]. The stress vectors at the electrode surface are parallel to the electric field vectors and their magnitude t_M is calculated from the electric field magnitude E or alternatively from the surface charge density ρ_s, see [3].

$$t_M = \frac{1}{2}\varepsilon_r\varepsilon_0 E^2 = \frac{\rho_s^2}{2\varepsilon_0\varepsilon_r} \tag{12}$$

In Fig. 7 the electrostatic stress distribution for the internal surface area $t_{M,i}$ and the lateral surface area $t_{M,l}$ are shown. For the calculation of $t_{M,l}$ the dielectric constant of vacuum ($\varepsilon_r = 1$) was used because the lateral surface area borders the empty space.

The stress for the internal surface area $t_{M,i}$ is constant with a singularity at the edge of the electrode. Singularities occur

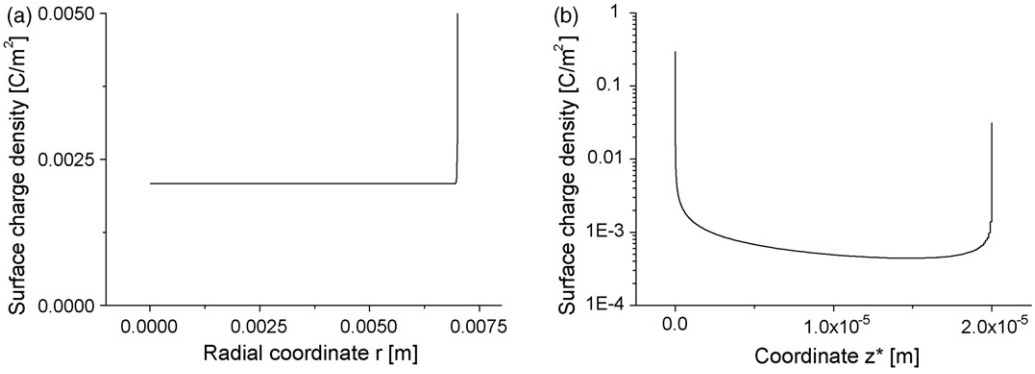

Fig. 5. Charge distributions on the electrode for (a) the internal surface area and (b) the lateral surface area.

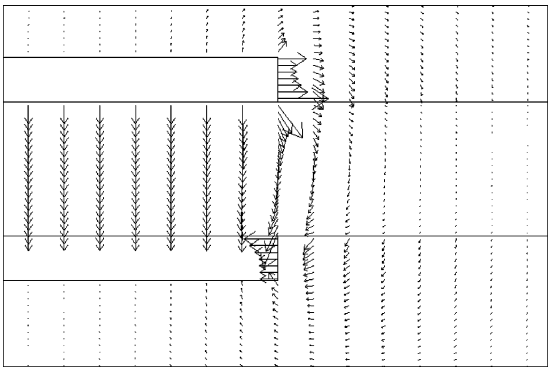

Fig. 6. Electric field distribution: arrows length is proportional to field intensity.

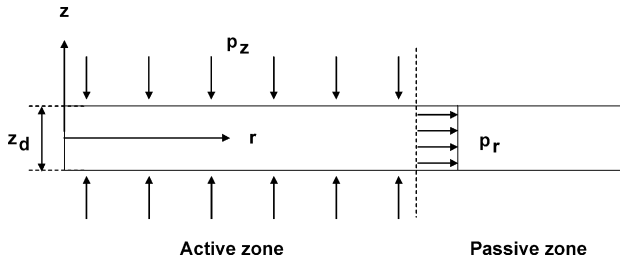

Fig. 8. Out-of-plane pressure p_z and lateral stress p_r acting on the dielectrica in a circular actuator, axisymmetric view.

also at the extremities of the lateral surface. Subsequent mesh refinement have shown that (i) the singularity for $t_{M,i}$ has no influence on the electromechanical behavior, and (ii) the value of the total radial force F_r from integration of $t_{M,l}$ over the thickness converges to a finite value.

The mechanical pressure p_z transmitted from the electrode to the dielectrica in (negative) z-direction (see Fig. 8) is constant over the coated area and has a value of $p_z = 52{,}018\ \mathrm{N/m^2}$.

The total force F_r caused by the Maxwell stress $t_{M,l}$ of the lateral surface area (see Fig. 3) is given by

$$F_r = \int_0^{z_{el}} 2\pi r_{el} t_{M,l}(z^*)\mathrm{d}z^* \tag{13}$$

F_r converges after mesh refinement to a value of 0.06784 N. As a simplification, $t_{M,l}$ can be replaced by a statically equivalent constant stress distribution in radial direction acting over the thickness of the elastomer film, see Fig. 8. The corresponding "lateral pressure" value (p_r, Fig. 8) is calculated taking into account the contribution of both electrodes (factor 2 in Eq. (14)):

$$p_r = 2\frac{F_r}{2\pi r_{el} z_d} = \frac{F_r}{\pi r_{el} z_d} \tag{14}$$

The calculated value of p_r for the applied mesh refinement is $51{,}415\ \mathrm{N/m^2}$.

The electromechanical pressure p_{el} calculated with Eq. (1) is, for the present case, $p_{el} = 104{,}036\ \mathrm{N/m^2}$.

This value is double as much as the calculated value of p_z and, with a slight approximation due to numerical errors, p_r.

$$p_z = p_r = \frac{1}{2}p_{el} = \frac{1}{2}\varepsilon_r\varepsilon_0\frac{U^2}{z_d^2} \tag{15}$$

This result shows that (i) the electrostatic forces act in out-of-plane and in-plane direction, and (ii) the out-of-plane component is half the value predicted with Pelrine's equation.

For an incompressible material, however, Pelrine's model can be shown to provide a suitable description of electromechanical coupling. In fact, a superimposed hydrostatic stress state does not affect, by definition, the deformation of the incompressible elastomer. For the present case a hydrostatic stress with negative sign and magnitude of $0.5p_{el}$ is superimposed to the vertical and radial components p_z and p_r. The resulting kinetic boundary condition is a homogeneous out-of-plane compression with p_{el}, i.e. the loading conditions predicted with Pelrine's model.

3. Dielectric constant

The analysis presented in Section 2 has confirmed that Eq. (1) can be used for modeling electromechanical coupling in DE systems. The value of the dielectric constant for VHB 4910 is investigated in this section. Several researchers [3,5,8,17,18], adopted a deformation independent value of about 4.7, originally proposed by Kofod et al. [10]. Different techniques were used here to measure ε_r for un-deformed and pre-stretched elastomer films.

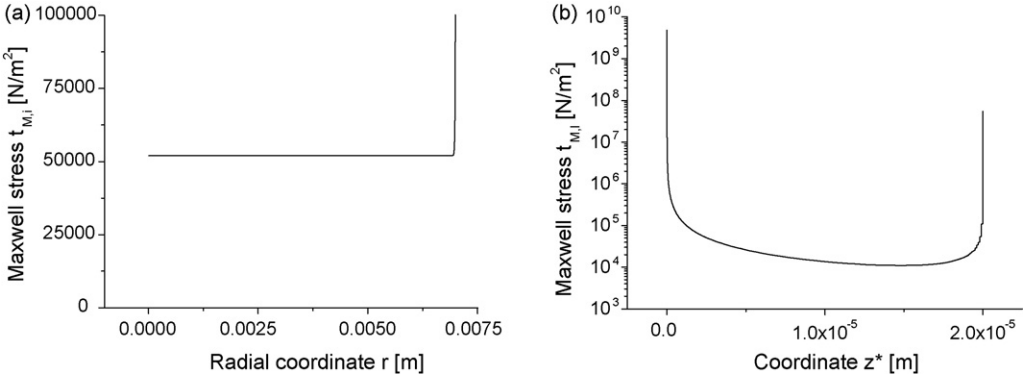

Fig. 7. Electrostatic stress distribution for (a) the internal surface area and (b) the lateral surface area.

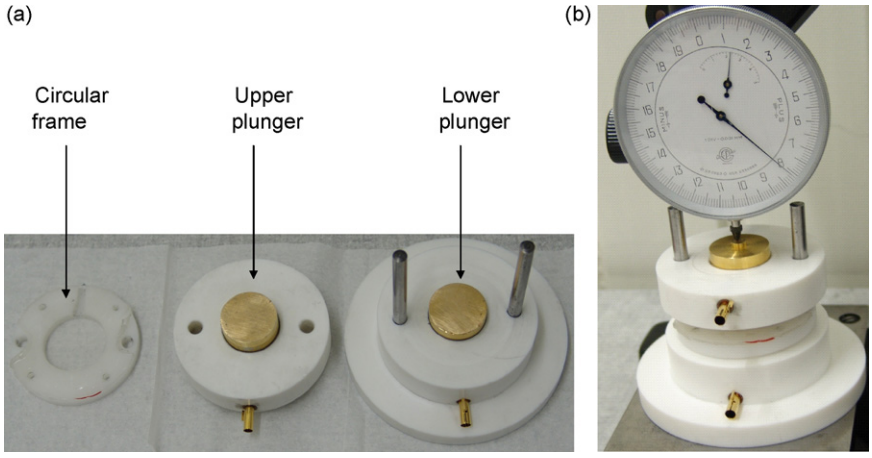

Fig. 9. Device for measuring the dielectric constant: (a) disassembled and (b) assembled device under the mechanical dial gage for thickness measurement.

3.1. Capacitor set-up

A capacitor set-up has been used to measure the dielectric constant of VHB 4910 at room temperature (23 °C). ε_r has been determined for different in-plane pre-stretch ratios ($\lambda_p = 1$, 3, 4 and 5) at the frequencies 100 Hz and 10 kHz. The dielectric constant can be obtained from measurements of capacitance and geometry of a capacitor:

$$\varepsilon_r = \frac{Cz}{A\varepsilon_0} \tag{16}$$

The elastomeric film is pre-deformed by a pre-stretching machine [8,19] and glued on a circular frame (radius 15 mm), Fig. 9. For each pre-stretch ratio five samples have been created for multiple measurements. Each sample is inserted between two gold plungers with a radius of 12.5 mm (Fig. 9). The capacitance is measured by a LCR-meter (an instrument for measuring the inductance (L), capacitance (C) and resistance (R), 4263B from Agilent) connected to two gold tubes (Fig. 9).

The thickness is measured by a mechanical dial gage (Compac, Switzerland, measurement range: 5 mm, resolution: 0.001 mm). The displacement of the upper capacitor plate is measured with and without the elastomer sample. The thickness corresponds to the displacement difference. The results of the dielectric constant are presented in Table 1 and Fig. 10.

Table 1
Dielectric constant (mean value ± standard deviation) for VHB 4910 at different frequencies and pre-strain levels

Pre-strain λ_p	ε_r at 100 Hz	ε_r at 10 kHz
1	4.68 ± 0.029	4.30 ± 0.025
3	3.71 ± 0.088	3.41 ± 0.098
4	3.34 ± 0.152	3.08 ± 0.184
5	2.62 ± 0.378	2.40 ± 0.410

3.2. "Spring roll" set-up

Dielectric constant measurements have been carried out using DE actuators in a cylindrical configuration, called "spring roll". Six spring rolls were manufactured and tested. The VHB 4910 membrane was coated with a mixture of graphite powder (Superior Graphite, ABG1005, 20 g) and silicone oil (Dow Corning, DC 200/50 cs, 45 g) as electrodes. A brief account on the actuator configuration is given below and detailed information can be found in [19].

The elastomer film is pre-strained biaxially (using the pre-stretching device [8,19]) with the pre-stretch ratios $\lambda_x = 4$ and $\lambda_y = 4$, see Fig. 11a. The pre-strained film is fixed to a rigid frame and one electrode is applied on one side (Fig. 11). The geometrical parameters after pre-straining are $x_1 = 143$ mm, $y_1 = 445$ mm

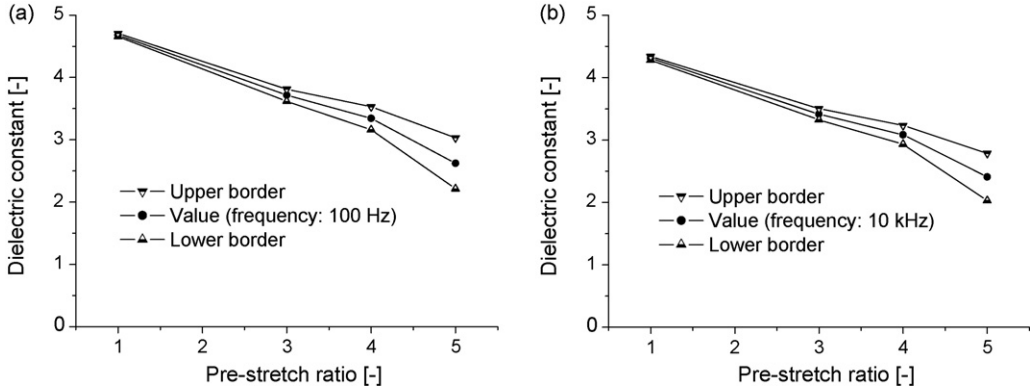

Fig. 10. Dielectric constant in dependence of the pre-stretch ratio (with scatter band) for (a) 100 Hz and (b) 10 kHz.

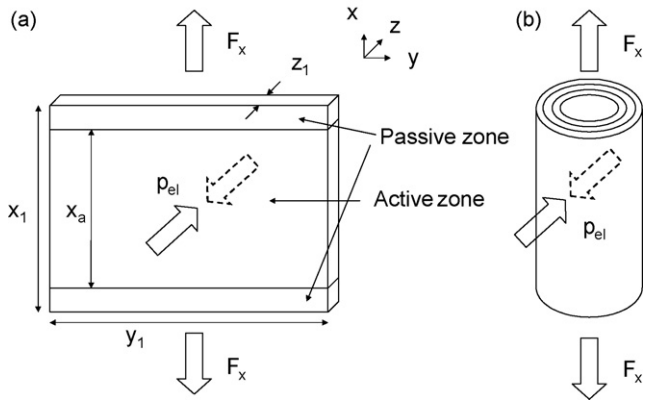

Fig. 11. (a) One layer (coated, pre-strained elastomer film) and (b) complete spring roll actuator.

and $z_1 = 62.5\ \mu m$. The coated (active) zone is in the middle of the actuator with $x_a = 110$ mm. The ratio r of the coated area divided by the whole area is $r = x_a/x_1 = 77\%$. A second layer consisting of the pre-stretched elastomer film and a second electrode is glued over the first layer at the uncoated side. Then, both layers are wrapped around an elastic core, Fig. 11.

The spring roll is hold at the extremities in x-direction by the force F_x. The experiment is performed at room temperature (23 °C). A voltage U is applied with a high voltage amplifier (Trek, Model 5/80) linearly increasing from 0 kV to 3 kV in 2 min. The force F_x required to keep the length of the actuator constant is continuously measured with a force transducer (HBM type S2). The experiment is controlled with a PC LabView system. The measured force difference ΔF is defined as

$$\Delta F(U) = F_x(U) - F_x(U = 0) \tag{17}$$

The actuators length remains unchanged despite the application of the voltage (and thus application of electrostatic forces). This means that the electrostatic forces together with the variation of axial stresses correspond to a hydrostatic stress state. As a consequence, measurement of the axial force (or the corresponding stress component) provides a direct measurement of the electrostatic stress:

$$p_{el} = \frac{\Delta F_i}{2x_1 y_1} = \varepsilon_0 \varepsilon_r E^2 \tag{18}$$

This equation allows determining the dielectric constant from the measurement of the force difference of an 'ideal' spring roll ΔF_i where the whole film is coated, $r = 100\%$. The present spring rolls have $r = 77\%$. The presence of passive parts (the remaining 23%) causes a deformation of the film with elongation in the coated and contraction in the uncoated area, Fig. 12. As a consequence, the change in axial force is somewhat lower with respect to the prediction according to Eq. (18). For describing the change in axial force the ratio k is introduced which is defined as $k = \Delta F/\Delta F_i$. The ratio k between force reduction with $r = 77\%$ and $r = 100\%$ has been evaluated analytically and numerically (finite element). The result of this analysis is that a constant value corresponding to the geometrical ratio (i.e. $k = r = 0.77$) represents a valid approximation for the present case. By using

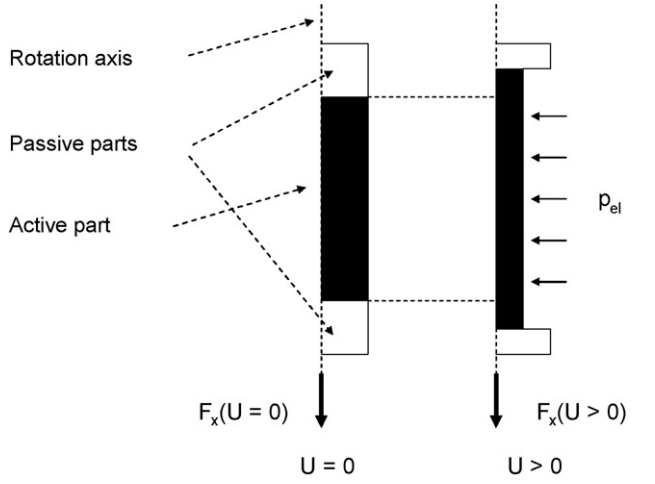

Fig. 12. Sketch to illustrate the influence of the passive parts on the spring roll behavior.

this result, Eq. (18) can be rewritten as:

$$p_{el} = \frac{\Delta F_i}{2x_1 y_1} = \frac{\Delta F}{2x_1 y_1 k} = \frac{\Delta F}{2x_1 y_1 r} = \varepsilon_0 \varepsilon_r E^2 \tag{19}$$

ε_r is evaluated by using Eq. (19). The electromechanical pressure $p_{el} = \Delta F/(2x_1 y_1 r)$ as a function of the electric field E is presented in Fig. 13. By fitting the experimental curve of p_{el} with Eq. (1), a dielectric constant of 3.24 is obtained. This result agrees to a great extent with the values reported in Table 1 for $\lambda_p = 4$.

4. Discussion

The analysis presented in Section 2 provides a validation of the Pelrine's equation for modeling electromechanical coupling in a circular actuator and a new interpretation of the electromechanical forces distribution. Energy and force considerations are consistent.

The energy balance considered here leads to the same result as in Pelrine et al. although the derivation is different. In fact, we considered the dependence of Q and U on the deformation.

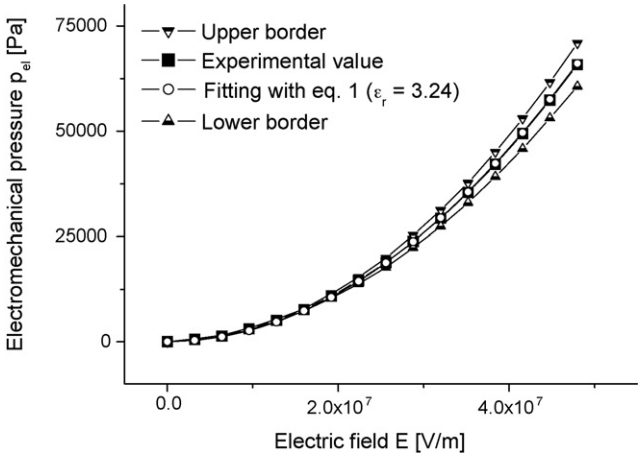

Fig. 13. Electromechanical pressure (with scatter band) evaluated by spring roll experiments compared to a fit with Eq. (1). The fitting parameter ε_r is 3.24.

As a consequence the derivatives dW_{ext}/dz and dW_{el}/dz depends on the voltage derivative dU/dz.

Electrostatic charge and force distribution calculations showed that half of the electromechanical pressure acts as out-of-plane compression and the other half as in-plane tension. The out-of-plane force corresponds to the one calculated for a standard parallel plate capacitor. Due to the incompressibility of the material, electromechanical coupling can be modeled with an out-of-plane pressure with magnitude p_{el} according to Eq. (1). This approach is advantageous in actuator modeling since only out-of plane forces have to be considered.

Note, the validity of Pelrine's equation for modeling dielectric elastomer actuators is not an implicitness. Consider for instance a spheric configuration ('ballon actuator', Fig. 14) with the radius of the elastomer r_s and the thickness of the elastomer z_s, $z_s \ll r_s$. The elastomer is pre-strained and is coated at the inner and the outer surface. The inner pressure of a gas (e.g. helium) maintains the pre-strain. The capacity is $C = \varepsilon_0 \varepsilon_r A_s / z_s$ where A_s is the surface area of the sphere. The charge is $Q = CU$ and the uniform surface charge density at the electrode is $\rho_s = Q/A_s = CU/A_s = \varepsilon_0 \varepsilon_r U/z_s$. Eq. (12) for the Maxwell stress gives $t_m = 0.5\varepsilon_0 \varepsilon_r (U/z_s)^2$. This is the half of the pressure that one would obtain by direct application of Pelrine's equation.

The results of the dielectric constant measurements show a remarkable dependence on the pre-strain and a weak dependence on the frequency. In the undeformed state (pre-strain $\lambda_p = 1$) the value of the dielectric constant is around 4.7 which is the commonly used value [10,11]. An increase of the pre-strain causes a significant decrease of the dielectric constant. For a relevant actuator pre-strain range (around $\lambda_p = 4$) the dielectric constant is close to 3.

The present results are in contrast to the findings in [10,11] where it is shown experimentally that the dielectric constant of VHB 4910 has a negligible dependence on pre-strain and frequency. A reason for the different outcome of the present tests might be in the material composition, which might have changed recently. Interestingly, in a 3 M data sheet [21] of November 2005 the dielectric constant of VHB 4910 is given as 3.21 for 1 kHz and 2.68 at 1 MHz.

The measurements with the capacitor set-up are confirmed by the experiment with the spring roll actuator. An evaluation of the dielectric constant for a biaxially pre-strained actuator ($\lambda_p = 4$) gives a value of 3.24, in agreement with the results of Section 3.1 where the dielectric constant at a pre-strain of $\lambda_p = 4$ was measured as 3.34 for 100 Hz and 3.08 for 10 kHz.

The results of the spring roll experiments confirm the validity of Pelrine's equation for DE actuator modeling. This is consistent with the experimental validation of electromechanical coupling by Kofod and Sommer-Larsen [4].

The stretching of the elastomer might cause an anisotropy of the dielectric constant. The fact that the dielectric constant decreases in thickness direction by stretching might cause a change of the dielectric constant in planar direction. Since the molecules align in planar direction by stretching, it is expected that the polarizability increases in planar direction and decreases in thickness direction. As a consequence an increase of the dielectric constant in planar direction is expected. With our set-up it is not possible to measure the dielectric constant in planar direction. In order to evaluate the influence of an anisotropic dielectric constant with respect to the electromechanical coupling, the numerical analysis has been repeated. Four calculations with COMSOL Multiphysics were carried out using the dielectric constant in a tensor form. Thereby, the dielectric constant in thickness direction $\varepsilon_{r,z}$ was set to $\varepsilon_{r,z} = 4.7$ in each calculation. The dielectric constant in radial direction $\varepsilon_{r,r}$ was varied with values of 4.7 (isotropic case), 6, 8 and 10. Results shows, that the surface charge distribution of the internal surface area and therefore the mechanical pressure p_z remains unchanged. In contrast, the surface charge distribution at the lateral surface area changes, which has an influence on the radial pressure p_r. In Fig. 15, the ratio p_r/p_z is plotted against the dielectric constant in radial direction, $\varepsilon_{r,r}$.

These results show that contributions of out-of-plane and radial pressure are equal only for the case of isotropic dielectric

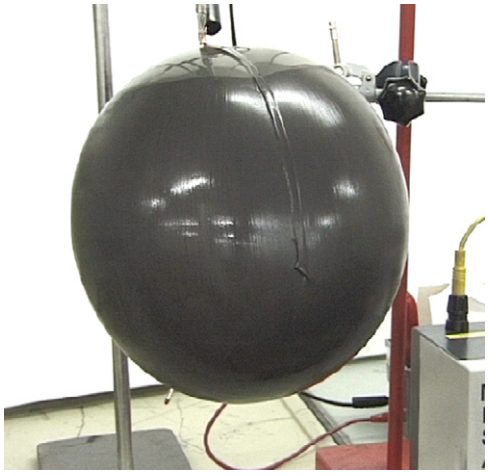

Fig. 14. Ballon actuator, taken from [20].

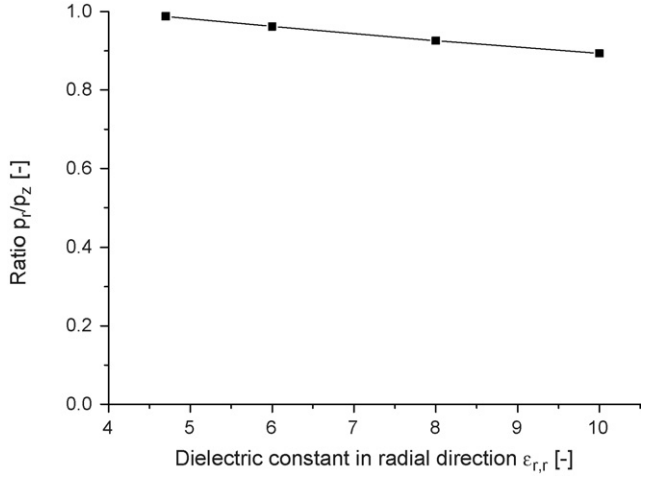

Fig. 15. The dielectric constant in radial direction $\varepsilon_{r,r}$ is plotted against the ratio p_r/p_z.

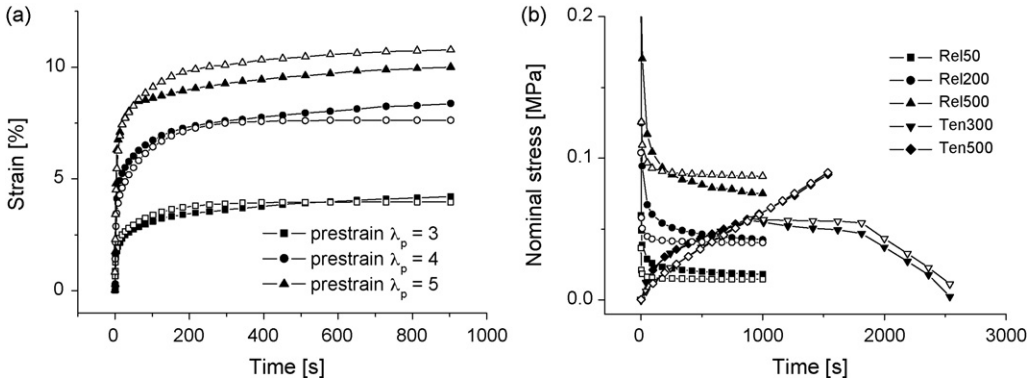

Fig. 16. Experiment vs. simulation for the same testing data points shown in Fig. 1: (a) circular actuator tests, and (b) uniaxial experiments. The filled symbols represent the experimental data and the open symbols the corresponding simulations, based on $\varepsilon_r = 3.24$.

behavior. With $\varepsilon_{r,r} = 10$ (more than double as $\varepsilon_{r,z} = 4.7$), the radial pressure p_r is 10% less as compared to the isotropic case. It can however be stated that the anisotropy of the dielectric constant has a small influence on the overall electromechanical behavior.

The results of Sections 2 and 3 showed that the Pelrine's equation can be used for circular actuator modeling but the dielectric constant has to be changed with respect to the value used in [8]. As a consequence, the results of the circular actuator experiments have been revisited and the constitutive model parameter identification corrected.

The circular actuators had pre-stretch ratios of $\lambda_p = 3, 4$ and 5. As a simplification, ε_r is not considered as pre-strain-dependent for the present analysis, and a constant value of $\varepsilon_r = 3.24$ has been selected, according to the value obtained for the spring roll actuator, see Fig. 12.

The new constitutive model parameters have been determined for the Arruda–Boyce strain energy form. In particular, the initial shear modulus (parameter A) is corrected with respect to [8], with $A = 0.0473$ MPa instead of 0.0686 MPa. Fig. 16 summarizes the new results for simulations of circulator tests and uniaxial response. The circular test fit is identical to the one reported in Fig. 1, and a significant improvement is obtained for the prediction of the uniaxial behavior.

5. Conclusions

Electromechanical coupling in DE actuator has been investigated. Validation of Pelrine's equation for modeling electromechanical coupling in circular actuators has been provided through (i) energy consideration and (ii) numerical calculation of charge and force distribution. The latter provided a new physical interpretation of the electrostatic forces acting on the DE film, with contributions from in-plane and out-of-plane stresses. Representation of this force distribution using Pelrine's equation is valid for an incompressible material, such as VHB 4910.

The value of the dielectric constant has been measured for different pre-stretched VHB 4910 membranes. The values are shown to decrease with increasing pre-stretch ratio, from 4.7 for the un-stretched film, down to 2.6 for a equi-biaxial deformation with $\lambda_p = 5$. This result is important in that it corrects the constant value of about 4.7 originally proposed in [10] and, since then, largely applied for pre-stretched DE actuator modeling, see e.g. [3,5,8,17,18]. The present values were obtained from a capacitor set-up and confirmed by the analysis of spring roll and circular actuator experiments.

Correction of the dielectric constant leads to a change in the VHB 4910 constitutive model parameters with respect to the values proposed in [8]. The new model is capable of describing the active and passive material behavior over a large range of loading conditions and deformation histories.

Acknowledgment

Financial support from the Swiss National Science Foundation (Project 200021-107661/1) is gratefully acknowledged.

References

[1] R.E. Pelrine, R.D. Kornbluh, J.P. Joseph, Electrostriction of polymer dielectrics with compliant electrodes as a means of actuation, Sensor. Actuators A 64 (1998) 77–85.
[2] R. Pelrine, R. Kornbluh, Q. Pei, J. Joseph, High-speed electrically actuated elastomers with strain greater than 100%, Science 287 (2000) 836–839.
[3] N. Goulbourne, E. Mockensturm, M. Frecker, A nonlinear model for dielectric elastomer membranes, J. Appl. Mech. 72 (2005) 899–906.
[4] G. Kofod, P. Sommer-Larsen, Silicone dielectric elastomer actuators: finite-elasticity model of actuation, Sensor. Actuators A 122 (2005) 273–283.
[5] J. Plante, S. Dubowsky, Large-scale failure modes of dielectric elastomer actuators, Int. J. Solids Struct. 43 (2006) 7727–7751.
[6] M. Wissler, E. Mazza, Modeling and simulation of dielectric elastomer actuators, Smart Mater. Struct. 14 (2005) 1396–1402.
[7] M. Wissler, E. Mazza, Modeling of a prestrained circular actuator made of dielectric elastomers, Sensor. Actuators A 120 (2005) 184–192.
[8] M. Wissler, E. Mazza, Mechanical behavior of an acrylic elastomer used in dielectric elastomer actuators, Sensor. Actuators A 134 (2007) 494–504.
[9] E.M. Arruda, M.C. Boyce, A three-dimensional constitutive model for the large stretch behavior of rubber elastic materials, J. Mech. Phys. Solids 41 (2) (1993) 389–412.
[10] G. Kofod, R. Kornbluh, R. Pelrine, P. Sommer-Larsen, Actuation response of polyacrylate dielectric elastomers, Proc. SPIE 4329 (2001) 141–147.
[11] G. Kofod, P. Sommer-Larsen, R. Kornbluh, R. Pelrine, Actuation response of polyacrylate dielectric elastomers, J. Intel. Mater. Syst. Struct. 14 (2003) 787–793.
[12] O.H. Yeoh, Characterization of elastic properties of carbon-black-filled rubber vulcanizates, Rubber Chem. Technol. 63 (1990) 792–805.

[13] R.W. Odgen, Large deformation isotropic elasticity—on the correlation of theory and experiment for incompressible rubberlike solids, Proc. R. Soc. Lond. A 326 (1972) 565–584.
[14] R. McMeeking, C. Landis, Electrostatic forces and stored energy for deformable dielectric materials, J. Appl. Mech. 72 (2005) 581–590.
[15] COMSOL Multiphysics, User's Guide, version 3.2, COMSOL, Inc., 2005.
[16] J.C. Maxwell, A Treatise on Electricity and Magnetism, Dover, Oxford, 1954.
[17] P. Lochmatter, S. Michel, G. Kovacs, Electromechanical model for static and dynamic activation of elementary dielectric elastomer actuators, Proc. SPIE 6168 (2006) 61680F-1–61680F-13.
[18] E. Yang, M. Frecker, E. Mockensturm, Viscoelastic model of dielectric elastomer membranes, Proc. SPIE 5759 (2005) 82–92.
[19] G. Kovacs, P. Lochmatter, Arm wrestling robot driven by dielectric elastomer actuators, Proc. SPIE 6168 (2006) 616807-1–1616807-12.
[20] P. Lochmatter, Develompent of a shell-like electroactive polymer (EAP) actuator, ETH dissertation, in preparation.
[21] http://www.mmm.com.

Biographies

Michael Wissler was born in Zurich, Switzerland in 1976. He graduated in material engineering at the Swiss Federal Institute of Technology (ETH) in 2002. He is a Ph.D. student in material engineering at the Swiss Federal Laboratories for Materials Testing and Research (EMPA). He works on modeling and simulation of polymer actuators.

Edoardo Mazza was born in 1969 in Sondrio (Italy). He studied mechanical engineering at ETH Zurich and received his Dr. sc. techn. degree at the ETH. After his Ph.D. he has been working in industry from 1997 to 2001. At Alstom Power he was group leader in the steam turbine R&D department and was responsible for the mechanical analysis of stationary and rotatory components. In November 2001 he was appointed as Assistant Professor for Mechanics at ETH Zurich. Since January 2006 he has been Associate Professor of Mechanics at the Institute of Mechanical Systems of ETH Zurich. His research deals with the solution of challenging continuum mechanics problems in modern engineering. Novel experimental techniques and constitutive models are developed for the characterization of the mechanical behavior of structures and materials.